Longitudinal In Vivo Monitoring of Atheroprogression in Hypercholesterolemic Mice Using Photoacoustic Imaging

Bartolo Ferraro[1,2,3]   Pierangela Giustetto[4,5]   Olga Schengel[6]   Ludwig T. Weckbach[2,3,7,8]
Lars Maegdefessel[2,9,10]   Oliver Soehnlein[1,2,6,11]

[1] Institute for Cardiovascular Prevention (IPEK), LMU Munich, Munich, Germany
[2] DZHK, Partner Site Munich Heart Alliance, Munich, Germany
[3] Institute of Cardiovascular Physiology and Pathophysiology, Biomedical Center, Ludwig- Maximilians-University Munich, Planegg-Martinsried, Germany
[4] Fujifilm VisualSonics Consultant, Amsterdam, The Netherlands
[5] Section of Physiology, Department of Biomedical and Biotechnological Sciences, University of Catania, Catania, Italy
[6] Institute for Experimental Pathology (ExPat), Centre for Molecular Biology of Inflammation (ZMBE), University of Münster, Münster, Germany
[7] Medizinische Klinik und Poliklinik I, Klinikum der Universität, Ludwig-Maximilians-University Munich, Munich, Germany

Address for correspondence Bartolo Ferraro, PhD, Biomedical Center LMU Munich, Großhaderner Straße 9, 82152 Planegg-Martinsried, Germany (e-mail: bartolo.ferraro@med.uni-muenchen.de).

[8] Walter Brendel Centre of Experimental Medicine, Ludwig-Maximilians-University Munich, University Hospital, Planegg-Martinsried, Germany
[9] Department of Vascular and Endovascular Surgery, Technical University Munich, Munich, Germany
[10] Department of Medicine, Karolinska Institutet, Stockholm, Sweden
[11] Department of Physiology and Pharmacology (FyFa), Karolinska Institutet, Stockholm, Sweden

Abstract

Background and Aim   The ability to recognize and monitor atherosclerotic lesion development using non-invasive imaging is crucial in preventive cardiology. The aim of the present study was to establish a protocol for longitudinal monitoring of plaque lipid, collagen, and macrophage burden as well as of endothelial permeability.

Methods and Results   Photoacoustic signals derived from endogenous or exogenous dyes assessed in vivo, in plaques of albino *Apoe*$^{-/-}$ mice, correlated with lesion characteristics obtained after histomorphometric and immunofluorescence analyses, thus supporting the validity of our protocol. Using models of atheroprogression and regression, we could apply our imaging protocol to the longitudinal observation of atherosclerotic lesion characteristics in mice.

Conclusions   The present study shows an innovative approach to assess arterial inflammation in a non-invasive fashion, applicable to longitudinal analyses of changes of atherosclerotic lesion composition. Such approach could prove important in the preclinical testing of therapeutic interventions in mice carrying pre-established lesions.

Keywords
► atherosclerosis
► inflammation
► photoacoustic imaging

Visual summary. Principle of the photoacoustic imaging used to simultaneously monitor, in a non-invasive way, lipids, collagen, Evans blue and XPLORE M800 deposition in the atherosclerotic lesions built in the brachiocephalic artery of albino Apoe$^{-/-}$ mice.

Introduction

Despite great advances in modern cardiovascular medicine, cardiovascular disease (CVD) remains the leading cause of morbidity and mortality worldwide.[1] The underlying pathological process of most CVDs is atherosclerosis, a chronic inflammatory disorder of large and medium-sized arteries that remain asymptomatic for decades. However, rupture of a vulnerable atherosclerotic plaque clinically manifests as myocardial infarction and stroke and hence identification of vulnerable lesions is a major goal of preventive cardiology.

Advanced atherosclerotic lesions are characterized by common features like a necrotic core, lipid-laden macrophages, and smooth muscle cells, as well as calcification and extracellular matrix deposition.[2] In addition, increased vascular permeability accelerates disease progression and lesion instability.[3] The onset of a coronary event is often triggered by the rupture of a vulnerable plaque, which sometimes might go undetected by conventional non-invasive diagnostic procedures.[4] Therefore, there is a need for new imaging methods or protocols allowing to detect plaque signs of vulnerability and to monitor these over time. Photoacoustic imaging (PAI) is an emerging imaging technique based on the photoacoustic effect. Briefly, nanosecond non-ionizing pulsed laser light is delivered into the tissue and part of the energy is absorbed by endogenous or exogenous chromophores, which causes local heating leading to transient tissue thermoelastic expansion and causing the emission of sound waves detected by an ultra-high frequency transducer.[5–7] PAI provides biochemical and functional information, physical characteristics, metabolic status, and pathological changes in a broad range of tissues; even though these features can also be assessed by intravascular near-infrared (NIR) fluorescence imaging, longitudinal imaging is limited by the invasiveness of this method.[8–10] To overcome this disadvantage, we present in our study a new protocol aimed at longitudinal monitoring traits of plaque inflammation and vulnerability. This method could also be helpful to test the effect of new therapeutic molecules on plaque stability.

Materials and Methods

Experimental Animals
All animal experiments were approved by the local ethics committee and performed in accordance with institutional regulations. In all experiments we used *Apoe*$^{-/-}$ mice intercrossed with C57BL/6J albino mice, the latter have a G-to-T base change at nucleotide 291 in the tyrosinase gene. In homozygous albino mice, pigment is completely absent from skin, hair, and eyes. In the first set of experiments, we used a cohort of old male and female mice fed a chow diet with an age range between 10 and 17 months. The idea to use such a cohort was to have mice with atherosclerotic lesions heterogeneous

in size and composition. In the second part of the study, we used a cohort of male mice (8–10 weeks old) randomly distributed in two experimental groups. The first group received high-fat diet (HFD; 21% fat, 0.15% cholesterol) for 18 weeks, while the second group received HFD for 12 weeks followed by 6 weeks of normal chow diet.

Phantom Preparation for In Vitro Characterization of Contrast Agents

To discriminate our endogenous molecules or the exogenous contrast agents of interest from other endogenous absorbers, we first characterized them in vitro under controlled conditions using a Vevo phantom imaging chamber (Visualsonics) and customized contrast agent phantom tubing (cat no. 52807, Visualsonics). We used polyethylene tubes with an inner diameter of 0.58 mm and an outer diameter of 0.965 mm positioned approximately 3 mm away from the ultra-high frequency transducer and embedded in a matrix of polyvinyl acetate in a saturated solution of sodium tetraborate decahydrate. The tubes, installed in the plastic phantom imaging chamber, were filled using a 27-gauge needle with dyes or molecules of interest to explore their spectral properties. The transducer was aligned perpendicular to the capillary tubes, and cross-sectional images along the tubes were acquired throughout the wavelength range (680–970 and 1,200–2,000 nm), with a step size of 5 nm. For some dyes we observed a deposition along the tube wall. For collagen spectral curve characterization, we filled the plastic tube using collagen type I from rat tail (Sigma-Aldrich cat. no C7661) solubilized in 0.1 M acetic acid solution at a final concentration of 1 mg/mL. For characterization of lipids, we extracted lipids directly from a pool of three aortic arches harvested from three $Apoe^{-/-}$ mice (9–10 months old) with established atherosclerotic lesions. For lipid extraction, we used a protocol adapted from the Folch method.[11] Briefly, 150 mg of tissue was disrupted with chloroform/methanol (2/1) to a final volume 20 times the volume of the tissue sample, using a tissue homogenizer (TissueLyser LT Qiagen). After dispersion, the entire mixture was agitated 1 hour on a shaker at room temperature and centrifuged at 1,500 rpm for 2 minutes to recover the liquid phase. The solvent was washed with water and after vortexing for 5 seconds, the mixture was centrifuged at a low speed (1,000 g for 10 minutes) to separate the two phases. The upper phase was discarded, and the lower phase was dried under the hood at 50°C and resuspended in 200 µL of isopropanol.

To assess macrophage content, we used a commercially available macrophage targeting contrast agent called XPLORE MΦ FL800 (iTheraMedical, cat no. XPL-MPH800). As reported by Kang et al,[12] the NIR probe CDnir7 (commercially XPLORE MΦ FL800) can selectively be taken up in vitro by the macrophage cell line Raw 264.7 and in vivo in a mouse model of acute inflammation obtained by injecting lipopolysaccharide (LPS) in the mouse paws. In detail, CDnir 7 injected via the tail vein and imaged after 30 minutes using IVIS spectrum imaging system accumulates specifically in the LPS injection sites. Immunostaining images showed that the dye colocalizes with macrophages at the sites of inflammation.

In our setting, XPLORE MΦ FL800 was freshly prepared according to the manufacturer protocol and 0.6 µg per gram of body weight was injected intravenously in each imaging session. To assess endothelial permeability, we used 1 mg of Evans Blue (Sigma-Aldrich cat no. E2129) dissolved in 100 µL of sterile phosphate-buffered saline (PBS). The dose was chosen from a previously published paper.[13] All measurements shown in the study were performed 1 hour after the intravenous injection of both exogenous dyes.

For each dye, we investigated the spectral curve using the spectro-mode which allows the rapid collection of photoacoustic data across the entire wavelength range (680–970 and 1,200–2,000 nm). These spectral curves were subsequently used to instruct the Vevo LAZR-X (VisualSonics, FUJIFILM, Toronto, Canada) how to recognize in vivo the photoacoustic signals of collagen and lipid content within the atherosclerotic region and exogenous dyes (Evans Blue and XPLORE MΦ FL800).

In a second set of experiments, the plastic tubes were filled with the same dyes as described above, and to mimic the in vivo scenario we positioned the plastic tubes approximately 5 mm away from the ultra-high frequency transducer and embedded in a tissue-mimicking matrix, a solution of PBS containing 1.3% agar powder (Sigma-Aldrich, cat. no 05040). Tissue-like scattering properties were introduced by mixing 12% of Intralipid 20% emulsion (Sigma-Aldrich, cat. no I141) to the agar.[14]

High-Resolution Ultrasound and Photoacoustic Imaging

To conduct longitudinal experiments, a high-resolution and high-frequency ultrasound (US) imaging system Vevo 3100 (VisualSonics, FUJIFILM, Toronto, Canada) equipped with a MX550D transducer was employed to acquire parasternal long-axis view two-dimensional (2D) and three-dimensional (3D) B-mode images or pulsed wave (PW) Doppler-mode images to measure plaque volume/area, lumen size, or pulse wave velocity (PWD), respectively. The transducer used for imaging has a central frequency of 40 MHz. For the imaging, the experimental mouse was anesthetized in an induction chamber using isoflurane 3% and 1 L/min oxygen for 1 to 2 minutes. When the mouse was under deep anesthesia, it was positioned supine on a heated platform to keep the body temperature stable. The mouse paws were fixed on the electrodes and the mouse was maintained under isoflurane anesthesia. Respiration rate, body temperature, heart rate as well as the electrocardiogram (ECG) were monitored during the entire imaging session. For the photoacoustic in vivo imaging of lipids and collagen content, we performed 2D and 3D scans in the 1,200 to 2,000 nm range using the Spectro and Multi wavelength modes. For Evans Blue and XPLORE MΦ FL800 in vivo PAI, we performed 2D and 3D scans in the 680 to 970 nm range after intravenous administration of the contrast agents using the same imaging modalities. Their accumulation in the atherosclerotic lesion was monitored for 1 hour.

All the measurements were performed using the VevoLab software version 3.2. PWD in the brachiocephalic artery was calculated indirectly using the formula: $PWV = D/[T_2 - T_1]$.[15]

The brachiocephalic artery distance was measured as D (mm) between the two sample volume positions, labeled as d_0 and d, respectively. The PW Doppler-mode sample volume was placed right after the atherosclerotic lesion and the time from the onset of the QRS complex to the onset of the ascending brachiocephalic artery Doppler wave form was measured as T_1. T_2 was calculated, placing the PW Doppler-mode sample volume as distal as possible in the same artery, as the time from the onset of the QRS complex to the onset of the ascending brachiocephalic artery Doppler wave form.

Histomorphometric and Immunofluorescence Analyses

After the final in vivo scan, the mouse was perfused, under deep anesthesia, by injecting 20 mL of PBS using a 30-gauge needle into the apex of the left ventricle and the aortic arch was harvested, again washed in PBS for 1 minute and fixed for 24 hours in paraformaldehyde 4% and subsequently embedded in a solution of 2% agarose (Agarose NEEO ultra-quality, Roth EG-Nr2327318). After 3D ex vivo imaging, the aortic arch was removed from the agarose matrix, embedded in Optimal cutting temperature compound (OCT) and cryosectioned in 4-µm slices. For immunofluorescence staining, tissue processing, antigen retrieval, and blocking of nonspecific staining were performed. Samples were incubated in primary antibody at 4°C overnight. After washing in PBS with Tween 20 (Millipore cat. no 9005–64–5), sections were incubated in the appropriate fluorescent-labeled secondary antibodies followed by counterstaining with DAPI and then mounted in ProLong Diamond Antifade Mountant (LifeTechnologies cat. no P36970). To stain plaque macrophages, we used an anti-Mac2 antibody (dilution 1:300, Cedarlane cat. no CL8942AP clone M3/38) and as a secondary antibody we used a Cy3-labeled anti-rat antibody (dilution 1:500, Jackson Immuno Research cat. no 712165150). For Sirius red staining of collagen, sections were incubated with 0.1% Sirius red (WALDECK GmbH & Co.) in saturated picric acid for 60 minutes. Afterward, they were incubated with 0.01 N HCl for 2 minutes and then dehydrated in ascending alcohol series and mounted with coverslips. Sections (3–5 chosen from proximal, middle, and distal parts of the atherosclerotic lesion) were photographed with identical exposure settings under ordinary light microscopy or fluorescence microscopy. For oil red O staining of lipids, PFA (paraformaldehyde)-fixed sections were stained in an Oil Red O solution for 15 minutes and counterstained with a Hematoxylin solution for 30 seconds. For Evans Blue, we performed an indirect quantification of endothelial cell activation staining the tissue with an anti-CD31 (dilution 1:50, Biolegend cat. no 102514, clone MEC 13.3) and an anti-VCAM-1 (dilution 1:100, R&D cat. no MAB6432 clone 112734) antibodies. For VCAM-1, we used a Cy3-labeled anti-rat antibody (dilution 1:500, Jackson Immuno Research cat. no 712165150) as a secondary antibody. For endothelial activation, we measured CD31/VCAM-1 costaining. We also directly imaged Evans Blue accumulation in the atherosclerotic lesion illuminating the sample with normal light since it is a visible dye. The stained area was measured using Image J 1.8v software. Representative

images showing Evans Blue (excitation at 620 nm, emission at 680 nm) extravasation in the atherosclerotic lesion were acquired using an upright confocal microscope (Examiner, Zeiss).

Statistics

Data are expressed as mean ± standard deviation. Statistical analyses were performed using GraphPad Prism 8. Statistical tests are specified in figure legends. p-Values < 0.05 were considered significant.

The D'Agostino–Pearson normality test was used to test distribution, while to identify outliers we used the ROUT method.

Results

In Vitro Characterization of Contrast Agents

To establish a new protocol for PAI of atherosclerotic lesions, we first evaluated in vitro the optical properties of the endogenous and exogenous contrast agents of interest. Spectral curves of lipids, collagen, Evans Blue, and XPLORE MΦ FL800 show specific absorption peaks important for the subsequent in vivo spectral unmixing of the dyes from all the other endogenous NIR absorbers (►**Fig. 1A**). Lipids and collagen absorption peaks fall in the NIR wavelength range of 1,200 to 2,000 nm (►**Fig. 1B, C**), while the two exogenous dyes absorb mainly in the range of 680 to 970 nm (►**Fig. 1D, E**). For control purposes, we repeated the experiment filling the plastic tubes only with the solvents used to dissolve the different molecules or dyes. Here, no specific absorption peaks were identified (►**Fig. 1F–J**). Using the spectro mode, we replicated the spectral curve for each dye in vivo, derived from a region of interest (ROI) drawn in a region enriched with the dye or molecule of interest (►**Supplementary Fig. S1A–D** [available in the online version]). The XPLORE MΦ FL800 spectral curve was perturbed in vivo by the hemoglobin NIR absorption properties, a phenomenon also observed in vitro when the dye was mixed 1:1 with mouse whole blood (data not shown). To get rid of any possible perturbance of the blood on our dye, the photoacoustic signal of oxygenated and deoxygenated hemoglobin was subtracted from the one detected for XPLORE MΦ FL800. PAI settings used for ex vivo and in vivo scans are shown in ►**Supplementary Tables S1** and **S2** [available in the online version], respectively.

Validation of In Vivo Characterization of Photoacoustic Imaging of Mouse Atherosclerotic Lesions

To prove that with this technology we can accurately measure the photoacoustic signal of the different molecules in vivo in the atherosclerotic plaque, we used a cohort of aged albino $Apoe^{-/-}$ mice with an age range between 10 and 17 months, thus exhibiting atherosclerotic plaques of different sizes and characteristics. Evans Blue, XPLORE MΦ FL800, lipids, and collagen accumulation were assessed in the brachiocephalic artery in vivo (►**Fig. 2A–D**) and ex vivo in the excised aortic arch (►**Fig. 2E–H**). The photoacoustic measurements obtained in vivo and ex vivo were compared with histology and immunohistochemistry, the current gold
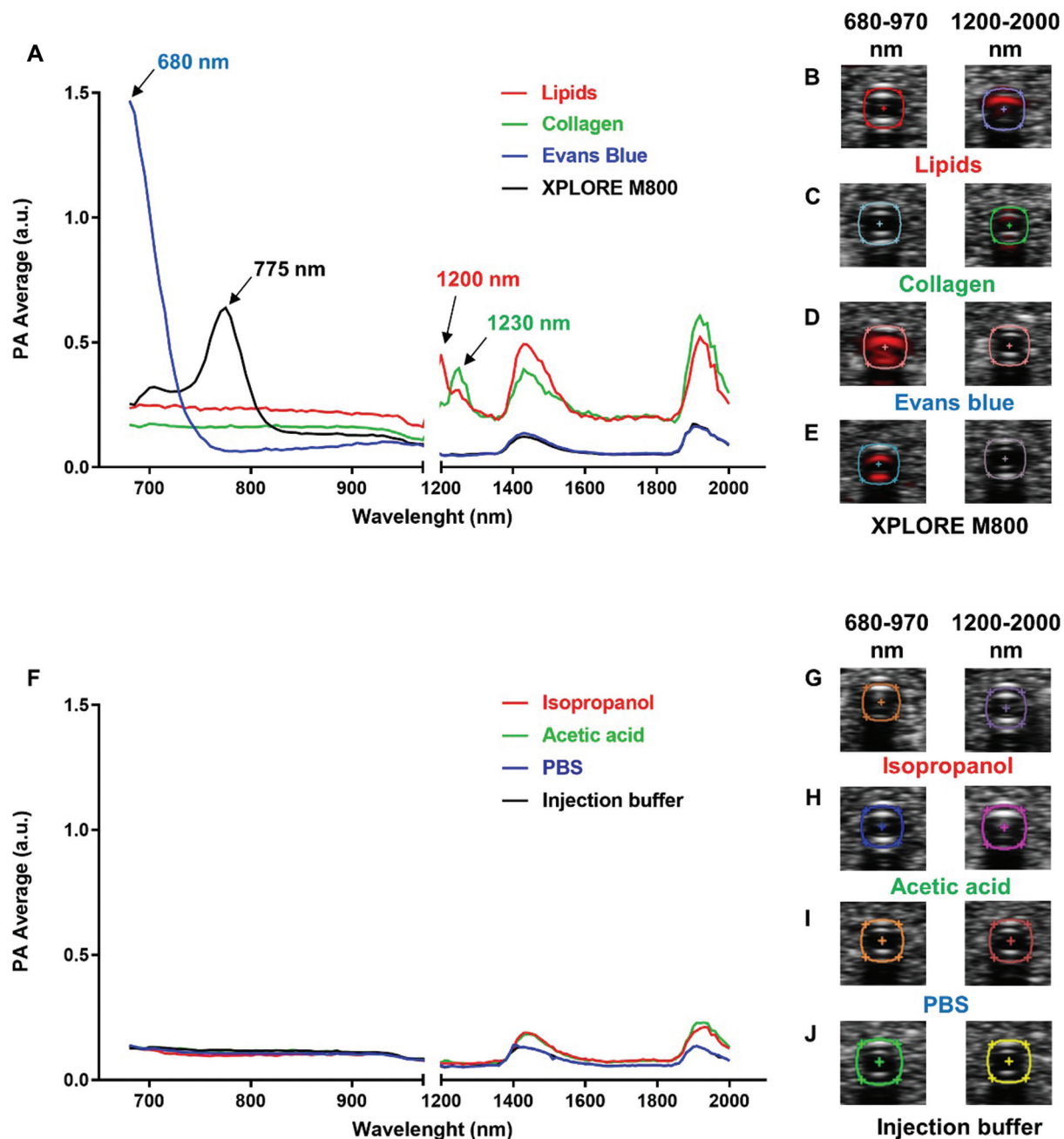
Fig. 1 In vitro dyes characterization. (A–E) Spectral curves generated in an ex vivo phantom from the average photoacoustic signal intensity in the region of interest and expressed as arbitrary units (a.u.), for Evans Blue, XPLORE MΦ FL800, lipids, and collagen. For each line the peak absorbance is indicated. Displayed is a merge of the optoacoustic image and B-Mode 2D image of plastic tubes containing lipids extracted from a pool of three aortic arches with atherosclerotic lesions (B), commercially available collagen Type I (1 mg/mL) (C), Evans Blue (1 mg dissolved in sterile PBS) (D), and XPLORE MΦ FL800 (E). The two images refer to the acquisition in two different windows of the near-infrared region. (F–J) Spectral curves generated in an ex vivo phantom for the solvents used to dissolve the different molecules or dyes and relative B-mode 2D image of the plastic tubes containing the solvents scanned in two different windows of the near-infrared region.

standard to characterize lesion composition in mice (►**Fig. 2I–P**, **U**, **V**). The procedure to match the ROI in vivo, ex vivo, and in histology was to measure the optoacoustic signal along 1 mm section of the brachiocephalic artery starting from the point where it intersects the ascending aorta. Examples of this procedure are shown in ►**Supplementary Fig. S2A–F** (available in the online version).

The photoacoustic signal measured in vivo significantly correlated with the signal obtained from the histological sections (►**Fig. 2Q–T** and **W**) as well as the photoacoustic signal measured ex vivo (►**Supplementary Fig. S3A–I** [available in the online version]). All the data shown for the correlations were normalized (min–max scaling). Taken together, these data suggest that our protocol can be successfully employed for in vivo imaging of lipids, collagen, Evans Blue, and macrophages in atherosclerotic prone regions.

With the intrinsic limitation of PAI to visualize deep structures, we positioned the plastic tubes at a depth of
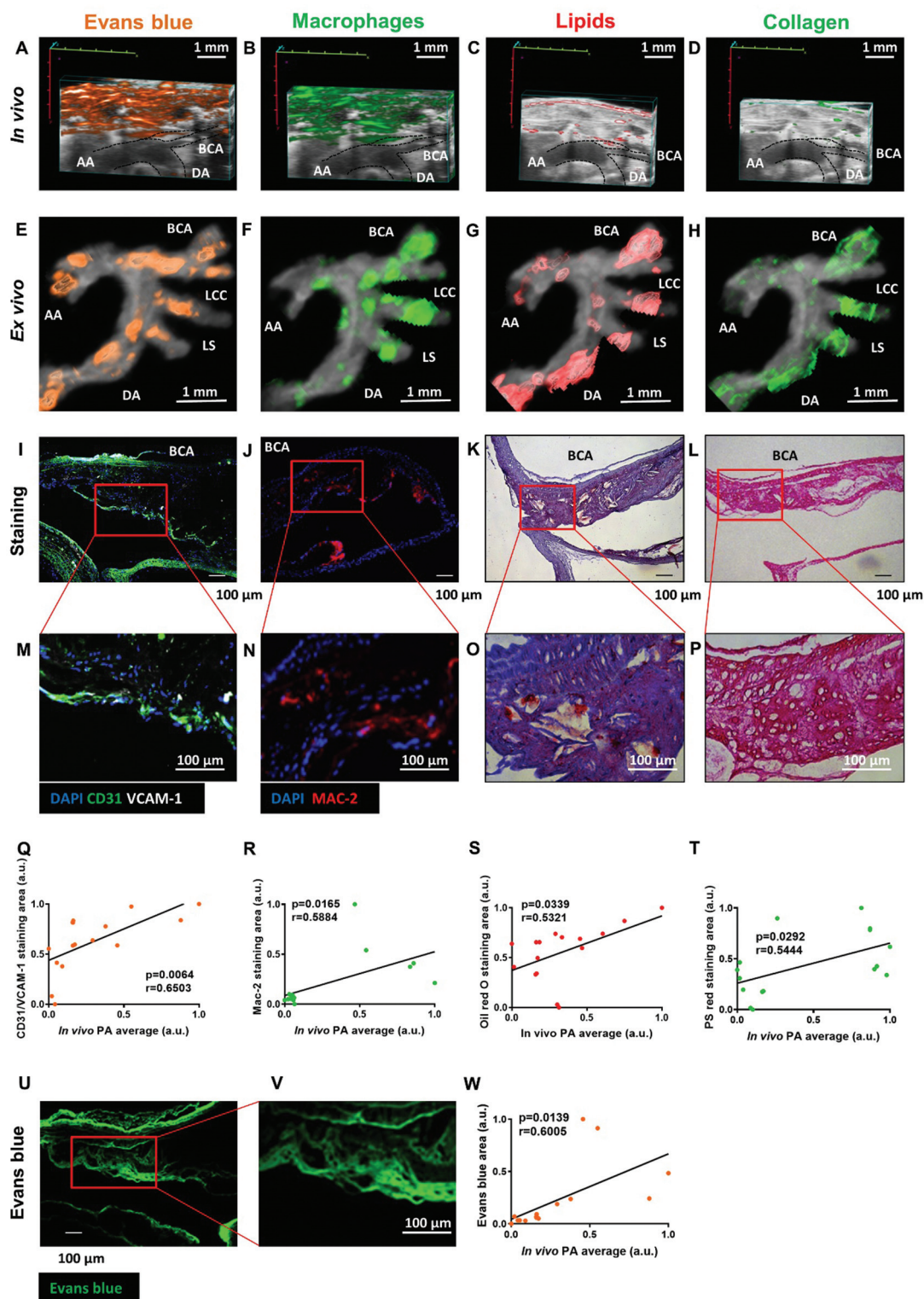
Fig. 2 Validation of in vivo characterization of photoacoustic imaging of mouse atherosclerotic lesions. (**A–D**) Representative images of the unmixed photoacoustic signal of Evans Blue, macrophages, lipids, and collagen, respectively, in 3D in vivo scans of a mouse bearing advanced lesions. (**E–H**) Representative images of the unmixed photoacoustic signal of the above-mentioned molecules or dyes, in 3D ex vivo scans of mice displayed in (**A–D**). (**I–P** and **U, V**) Representative images and relative zoom-in images of aortic arch sections obtained from mice displayed in (**A–D**). Endothelial permeability was assessed indirectly by staining the tissue using antibodies to CD31 and VCAM-1 to assess endothelial cell activation and directly visualizing and measuring Evans Blue extravasation in the atherosclerotic lesion. Macrophages were visualized by anti-Mac2 staining, oil-red O and picrosirius red staining were used to visualize lipids and collagen, respectively. (**Q–T** and **W**) Correlation between the photoacoustic signal measured in vivo and in stained histological sections (Pearson correlation, $n = 16$). All the data shown were normalized (min–max scaling). AA, ascending aorta; BCA, brachiocephalic artery; DA, descending aorta; LCC, left common carotid artery; LS, left subclavian artery.

approximately 5 mm recapitulating the positioning of the atherosclerotic plaque of our interest within a mouse and repeated the in vitro imaging of all contrast agents (►**Supplementary Fig. S4A–D** [available in the online version]). The tubes were embedded in a tissue-mimicking matrix, a solution obtained mixing agar and Intralipid 20% emulsion. In this setting, we were still able to pick up the photoacoustic signals derived from the different dyes although its amplitude was slightly decreased compared with ►**Fig. 1A** (►**Supplementary Fig. S4E** [available in the online version]). To further validate the usefulness of the two exogenous tracers in detecting atherosclerotic lesions, we performed pre- and postinjection scans in an old Apoe$^{-/-}$ mouse (►**Supplementary Fig. S5A, B** [available in the online version]). We also performed in vivo and ex vivo 3D scans of an old wild-type mouse (14 months old) used as a negative control. In this mouse, no signals for lipids and collagen as well as for Evans Blue and XPLORE MΦ FL800, 1 hour after the intravenous injection of the two dyes, were observed in the aortic arch (►**Supplementary Fig. S5C–F** [available in the online version]). As a positive control for lipids and collagen deposition, we repeated the 3D imaging on a piece of liver harvested from an Apoe$^{-/-}$ mouse fed with HFD for 14 weeks (►**Supplementary Fig. S5G, H** [available in the online version]).

Longitudinal In Vivo Photoacoustic Imaging of Mouse Atherosclerosis

The second part of the project was aimed to prove that our protocol can be applied longitudinally to monitor changes in plaque composition over time. To this end, we used a cohort of young albino *Apoe*$^{-/-}$ mice and randomly distributed them in two experimental groups. The first group received HFD (21% fat, 0.15% cholesterol) for 18 weeks (►**Fig. 3A**), while the second group received HFD for 12 weeks followed by 6 weeks of normal chow diet (►**Fig. 3K**). The mice were scanned after 12 and 18 weeks to assess changes in plaque composition and size. In the first experimental group, we observed that continued HFD feeding promotes a significant increase of lipids, collagen content, and a tendency toward heightened endothelial permeability (►**Fig. 3B–D**, **F**). In contrast, we noted no significant change in macrophage accumulation (►**Fig. 3E, F**). In the second experimental group, switching the diet after 12 weeks of HFD to normal chow diet led to a significant decrease in transendothelial permeability (►**Fig. 3N, P**), while lesional content in lipids, collagen, and macrophages remained unchanged (►**Fig. 3L, M, O, P**). In addition, volume calculations of the ROI drawn around the atherosclerotic lesion show that there is no difference in the volume of the ROI used for photoacoustic signal measurements overtime (►**Supplementary Fig. S6A–L** [available in the online version]). For both experimental groups, we also measured the plaque volume which was significantly increased overtime during the HFD regimen (►**Fig. 3H, I**), but it only slightly decreases after diet switching (►**Fig. 3R, S**). As a consequence of plaque growth, for the first group we observed a significant reduction in the lumen size of the brachiocephalic artery

(►**Supplementary Figs. S3G** and **S7A–F** [available in the online version]) and an increase in PWD in the same vessel (►**Supplementary Figs. S3J** and **S7A–F** [available in the online version]); while in the second group, we noted no change in lumen size or PWD (►**Supplementary Figs. S3Q, T** and ►**Fig. S7A–F** [available in the online version]).

Discussion

To date several biomedical imaging modalities such as US, computed tomography angiography (CTA), and magnetic resonance (MR) angiography have been routinely used alone or in combination to investigate atherosclerotic plaque burden and composition. Even though all these imaging techniques provide morphological and functional information, all have inherent limitations including poor sensitivity, low spatial resolution, use of harmful ionizing radiation or iodinated contrast agents, slow imaging speed, high costs, and patient discomfort.[16] In this study, we present a new protocol to monitor features of plaque inflammation over time using PAI. PAI is an excellent imaging diagnostic tool because it uses non-ionizing radiation to image tissue with a high spatial resolution and contrast and long penetration depth; in addition, it provides real-time imaging capability, low costs, and little discomfort for the patient. PAI has been used in the last years to improve preclinical and clinical imaging, exploiting the intrinsic properties of several endogenous molecules such as lipids, collagen, water, melanin, and hemoglobin to absorb and emit light in the NIR region.[17] This methodology is also used to investigate many other molecules without the above-mentioned properties targeting them with exogenous NIR photoabsorbing probes.[17,18]

Many studies showed that it is possible to monitor lipid accumulation in different tissues especially based on the absorption peak at 1,200 nm due to the abundant C–H bonds, at which the absorption coefficients of lipids and oils are higher than that of water.[19,20] The absorption spectrum of collagen, an important component of the extracellular matrix whose amount and organization are associated with plaque stability, has also been extensively investigated over the last years with the advantage of high penetration depth and enhanced constituent specificity in the short-wave infrared (1,100–1,700 nm) range.[21,22] In our study, we were able to recapitulate in vitro but also in vivo the absorption peaks previously reported for lipids and collagen. Of note, we were able to distinguish lipids from collagen because collagen showed a peak around 1,230 nm, while lipids peaked at 1,200 nm.

Macrophage accumulation is another important feature linked to atherosclerotic plaque inflammation. Macrophage imaging has so far been conducted by isolating and labeling these cells ex vivo or by intravenous injection of contrast agents able to target them in inflamed tissues.[23] Ultrasmall superparamagnetic particles of iron oxide, for example, have been extensively used to detect inflammation using cardiovascular MR due to their ability to be uptaken through different mechanisms by inflammatory cells.[24] In our experiments, to target macrophages, we used a commercially available probe named CDnir7 or XPLORE MΦ FL800, which
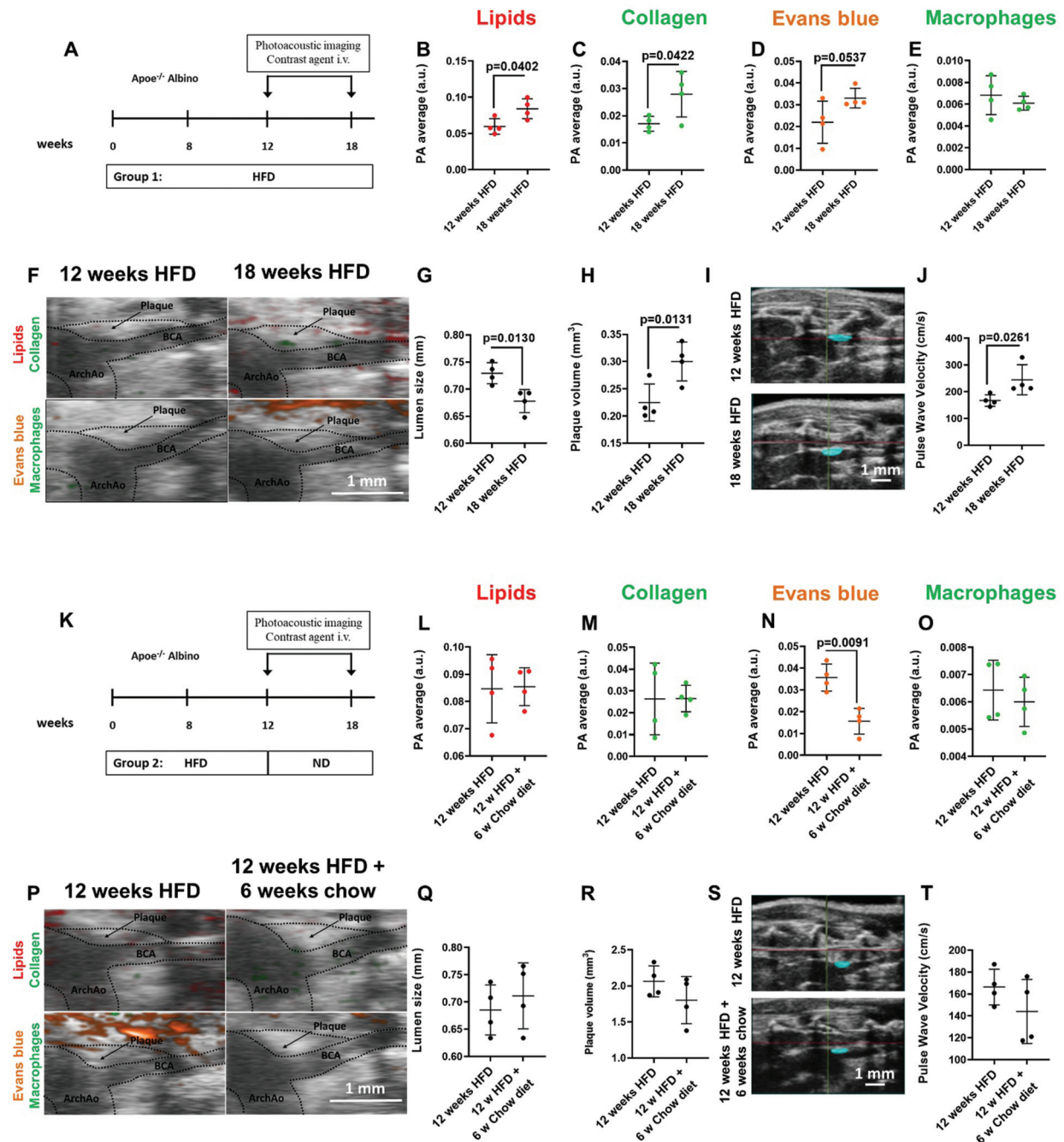
Fig. 3 Longitudinal in vivo quantification of lipids, collagen, endothelial permeability, and macrophage accumulation. (**A**) Experimental layout: the first group of albino $Apoe^{-/-}$ mice was fed with high fat diet (HFD) for 18 weeks. Longitudinal photoacoustic and echocardiographic scans were recorded after 12 and 18 weeks. (**B, C**) Quantification of lipids and collagen photoacoustic signal, calculated using the VevoLab 3.2 software in a ROI drawn around the atherosclerotic lesion build up in the region where the brachiocephalic artery (BCA) originates from the ascending aorta. (**D, E**) Quantification of Evans Blue and XPLORE MΦ FL800 photoacoustic signal measured at 12 weeks HFD and at 18 weeks HFD. (**F**) Representative images of lipids/collagen (top) and Evans Blue/macrophage (bottom) signal at the 12 week (left) and the 18 week (right) time point. (**G**) Brachiocephalic artery lumen size. (**H, I**) Plaque volume as assessed by 3D in vivo scans of lesions in the BCA. Representative images showing plaque size measurements after 12 and 18 weeks HFD (I). (**J**) Pulsed wave velocity measurements. (**K**) Experimental layout: the second group of albino $Apoe^{-/-}$ mice was fed with HFD for 12 weeks, subsequently they received chow diet for additional 6 weeks. Longitudinal photoacoustic and echocardiographic scans were recorded after 12 and 18 weeks. (**L, M**) Quantification of lipids and collagen photoacoustic signal, calculated using the VevoLab 3.2 software in a ROI drawn around the atherosclerotic lesion build up in the region where the BCA originates from the ascending aorta. (**N, O**) Quantification of Evans Blue and XPLORE MΦ FL800 photoacoustic signal measured at 12 weeks HFD and at 18 weeks HFD. (**P**) Representative images of lipids/collagen (top) and Evans Blue/macrophage (bottom) signal at the 12 week (left) and the 18 week (right) time point. (**Q**) Brachiocephalic artery lumen size. (**R, S**) Plaque volume as assessed by 3D in vivo scans of lesions in the BCA. Representative images showing plaque size measurements after 12 and 18 weeks HFD (S). (**T**) Pulsed wave velocity measurements. All data are mean ± SD. Each dot represents one mouse ($n = 4$). Paired t-test. ROI, region of interest.

has been previously shown to be selectively uptaken by macrophages both in vitro and in vivo in a mouse model of acute inflammation obtained by injecting LPS in the mouse paw.[12] The last characteristic we aimed to study was the loss of endothelial barrier function. To this end, we injected the plasma albumin marker Evans Blue which tends to accumulate in atheroprone regions and can be detected using PAI.[13]

The data obtained in the first part of the study show a significant correlation between the in vivo/ex vivo signal derived from the four different above-mentioned dyes and the signal observed in the histological sections, measured in the atherosclerotic region. In the second part of the study, we prove that this protocol can be applied longitudinally to monitor plaque progression over time. In particular, the photoacoustic scans revealed, in the group of mice fed with HFD for 18 weeks, an increased lipid and collagen accumulation in the plaque as well as an increased permeability of the endothelium compared with the group of mice subjected to a change of the dietary regimen during the last 6 weeks.

There are few limitations observed in our study. The first limitation, associated with the PAI technology, is the penetration depth, which allowed us to gain information only from the atherosclerotic lesions built in the brachiocephalic artery but not from those located deeper in the mouse chest. The second issue was to observe that the blood perturbates the spectral curve of the XPLORE M800 dye in vitro and to a less extend in vivo. To get rid of any possible perturbance of the blood on our dye, as previously described, the photoacoustic signal of oxygenated and deoxygenated hemoglobin was subtracted from the one detected for XPLORE MΦ FL800. Lastly, the sample size used for the longitudinal experiment represents another limitation of our study.

The strength of our protocol is the multimodal, simultaneous assessment of several different characteristics inherent to arterial inflammation besides those obtained from the echocardiographic imaging. In addition, the large array of available exogenous probes offers the possibility to further expand the amount of information about the atherosclerotic plaque status exploring key molecular mechanisms such as protease activity or cellular death.[25]

In a recently published preliminary study, researchers demonstrated, using a hybrid hand-held multi-spectral optoacoustic tomography/US system, the feasibility of resolving lipid and hemoglobin content in atherosclerotic plaques of a cohort of five patients with a diagnosis of carotid atherosclerosis.[26] In the same paper, the authors also describe several limitations linked to the PAI, such as the penetration depth, which they report to be approximately 2 to 4 cm due to light attenuation with increasing depth (via scattering and absorption), which is low compared with currently used modalities for carotid imaging such as US imaging, MR imaging, and CTA. Spectral unmixing as well as motion contamination also remains a challenging problem. They conclude that further technical developments are required in the fields of laser illumination, light attenuation compensation, and motion correction to be able to image vessels and anatomical districts located deeper in the human body.

If we compare our results to this study, we believe that our protocol, with the advantage of a non-invasive monitoring of atherosclerotic plaque composition over time, would represent an excellent tool for studying atherosclerosis in preclinical research.

What is known about this topic?

- Photoacoustic imaging is an excellent imaging diagnostic tool used in the last years to improve preclinical and clinical imaging, exploiting the intrinsic properties of several endogenous molecules such as lipids, collagen, and hemoglobin to absorb and emit light in the near-infrared (NIR) region.
- This imaging modality is also used to investigate many other molecules or biological processes using exogenous NIR photoabsorbing probes.

What does this paper add?

- An innovative non-invasive approach for in vivo simultaneous imaging of lipids, collagen, macrophage content, and endothelial permeability in murine atherosclerotic lesions.
- Longitudinal monitoring of atherosclerotic plaque composition.

References

1 Widmer RJ, Flammer AJ, Lerman LO, Lerman A. The Mediterranean diet, its components, and cardiovascular disease. Am J Med 2015;128(03):229–238
2 Hansson GK, Hermansson A. The immune system in atherosclerosis. Nat Immunol 2011;12(03):204–212

3 Phinikaridou A, Andia ME, Lavin B, Smith A, Saha P, Botnar RM. Increased vascular permeability measured with an albumin-binding magnetic resonance contrast agent is a surrogate marker of rupture-prone atherosclerotic plaque. Circ Cardiovasc Imaging 2016;9(12):e004910

4 Yeager D, Chen YS, Litovsky S, Emelianov S. Intravascular photoacoustics for image-guidance and temperature monitoring during plasmonic photothermal therapy of atherosclerotic plaques: a feasibility study. Theranostics 2013;4(01):36–46

5 Lemaster JE, Jokerst JV. What is new in nanoparticle-based photoacoustic imaging? Wiley Interdiscip Rev Nanomed Nanobiotechnol 2017;9(01). Doi: 10.1002/wnan.1404

6 Wang LV, Hu S. Photoacoustic tomography: in vivo imaging from organelles to organs. Science 2012;335(6075):1458–1462

7 Zackrisson S, van de Ven SMWY, Gambhir SS. Light in and sound out: emerging translational strategies for photoacoustic imaging. Cancer Res 2014;74(04):979–1004

8 Wu D, Huang L, Jiang MS, Jiang H. Contrast agents for photoacoustic and thermoacoustic imaging: a review. Int J Mol Sci 2014;15(12):23616–23639

9 Karlas A, Fasoula NA, Paul-Yuan K, et al. Cardiovascular optoacoustics: from mice to men - a review. Photoacoustics 2019;14:19–30

10 Hui J, Cao Y, Zhang Y, et al. Real-time intravascular photoacoustic-ultrasound imaging of lipid-laden plaque in human coronary artery at 16 frames per second. Sci Rep 2017;7(01):1417

11 Folch J, Lees M, Sloane Stanley GH. A simple method for the isolation and purification of total lipides from animal tissues. J Biol Chem 1957;226(01):497–509

12 Kang NY, Park SJ, Ang XW, et al. A macrophage uptaking near-infrared chemical probe CDnir7 for in vivo imaging of inflammation. Chem Commun (Camb) 2014;50(50):6589–6591

13 Lundeberg E, Van Der Does AM, Kenne E, Soehnlein O, Lindbom L. Assessing large-vessel endothelial permeability using near-infrared fluorescence imaging–brief report. Arterioscler Thromb Vasc Biol 2015;35(04):783–786

14 Razansky D, Harlaar NJ, Hillebrands JL, et al. Multispectral optoacoustic tomography of matrix metalloproteinase activity in vulnerable human carotid plaques. Mol Imaging Biol 2012;14 (03):277–285

15 Cui JZ, Lee L, Sheng X, et al. In vivo characterization of doxycycline-mediated protection of aortic function and structure in a mouse model of Marfan syndrome-associated aortic aneurysm. Sci Rep 2019;9(01):2071

16 Park S, Jung U, Lee S, Lee D, Kim C. Contrast-enhanced dual mode imaging: photoacoustic imaging plus more. Biomed Eng Lett 2017;7(02):121–133

17 Weber J, Beard PC, Bohndiek SE. Contrast agents for molecular photoacoustic imaging. Nat Methods 2016;13(08):639–650

18 Gujrati V, Mishra A, Ntziachristos V. Molecular imaging probes for multi-spectral optoacoustic tomography. Chem Commun (Camb) 2017;53(34):4653–4672

19 Zhang J, Yang S, Ji X, Zhou Q, Xing D. Characterization of lipid-rich aortic plaques by intravascular photoacoustic tomography: ex vivo and in vivo validation in a rabbit atherosclerosis model with histologic correlation. J Am Coll Cardiol 2014;64(04): 385–390

20 Jansen K, Wu M, van der Steen AF, van Soest G. Photoacoustic imaging of human coronary atherosclerosis in two spectral bands. Photoacoustics 2013;2(01):12–20

21 Sekar SK, Bargigia I, Mora AD, et al. Diffuse optical characterization of collagen absorption from 500 to 1700 nm. J Biomed Opt 2017;22(01):15006

22 Park E, Lee YJ, Lee C, Eom TJ. Effective photoacoustic absorption spectrum for collagen-based tissue imaging. J Biomed Opt 2020; 25(05):1–8

23 Park SJ, Kim B, Choi S, et al. Imaging inflammation using an activated macrophage probe with Slc18b1 as the activation-selective gating target. Nat Commun 2019;10(01):1111

24 Alam SR, Stirrat C, Richards J, et al. Vascular and plaque imaging with ultrasmall superparamagnetic particles of iron oxide. J Cardiovasc Magn Reson 2015;17(01):83

25 Tsang VTC, Li X, Wong TTW. A review of endogenous and exogenous contrast agents used in photoacoustic tomography with different sensing configurations. Sensors (Basel) 2020;20(19): 5595

26 Karlas A, Kallmayer M, Bariotakis M, et al. Multispectral optoacoustic tomography of lipid and hemoglobin contrast in human carotid atherosclerosis. Photoacoustics 2021;23:100283